Nanographene

Deutsche Ausgabe: DOI: 10.1002/ange.201606440
Internationale Ausgabe: DOI: 10.1002/anie.201606440

Aryl Radical Geometry Determines Nanographene Formation on Au(111)

Peter H. Jacobse, Adri van den Hoogenband, Marc-Etienne Moret, Robertus J. M. Klein Gebbink, and Ingmar Swart**

Abstract: *The Ullmann coupling has been used extensively as a synthetic tool for the formation of C–C bonds on surfaces. Thus far, most syntheses made use of aryl bromides or aryl iodides. We investigated the applicability of an aryl chloride in the bottom-up assembly of graphene nanoribbons. Specifically, the reactions of 10,10′-dichloro-9,9′-bianthryl (DCBA) on Au(111) were studied. Using atomic resolution non-contact AFM, the structure of various coupling products and intermediates were resolved, allowing us to reveal the important role of the geometry of the intermediate aryl radicals in the formation mechanism. For the aryl chloride, cyclodehydrogenation occurs before dehalogenation and polymerization. Due to their geometry, the planar bisanthene radicals display a different coupling behavior compared to the staggered bianthryl radicals formed when aryl bromides are used. This results in oligo- and polybisanthenes with predominantly fluoranthene-type connections.*

The Ullmann coupling has proven to be an indispensable tool for the bottom-up assembly of graphene nanostructures and covalent organic frameworks on surfaces.[1] Numerous structures can be accessed with aryl chlorides,[2] aryl bromides[3] and aryl iodides.[4] The combination of different halogen substituents in a single molecule has been used to provide an extra degree of freedom as individual Ullmann couplings can be carried out in sequence.[5] This hierarchical approach is also useful in the preparation of precursor molecules, which are typically synthesized by means of solution-based coupling methods. The presence of two different halogens then allows for solution-phase coupling on the heaviest halogen, followed by surface-mediated Ullmann coupling on the lightest one, providing increased synthetic freedom.

Among the most fascinating structures produced with the Ullmann coupling are graphene nanoribbons (GNR). The archetypical synthesis, pioneered by Cai et al., uses the precursor molecule 10,10′-dibromo-9,9′-bianthryl (DBBA).[6] The coupling is a two-step process, in which first the carbon–halogen bonds are dissociated thermally and the resulting (surface-bound) bianthryl radicals polymerize to give polyanthrylene.[7] By heating the polyanthrylene chains to over 250 °C, cyclodehydrogenation (CDH) is induced, transforming the staggered polyanthrylenes into flat, conjugated nanoribbons.[8] CDH releases hydrogen atoms onto the surface, which has been shown to passivate leftover radicals.[9]

Nanoribbons of various widths, edge structures, and heteroatom-functionalized GNRs have been synthesized.[10] Interestingly, all of the precursor molecules were synthesized by means of aryl halide coupling chemistry. The subsequent on-surface synthesis has so far also always employed the aryl bromide Ullmann coupling. Investigating the feasibility of aryl chloride Ullmann coupling in the on-surface synthesis of GNR is highly desirable as it may increase the flexibility and selectivity of the solution-phase synthesis of the precursor molecules.

Here, we report on our investigation of the applicability of the aryl chloride Ullmann coupling in the thermal assembly of graphene nanostructures. Specifically, the precursor 10,10′-dichloro-9,9′-bianthryl (DCBA) was used, which is the chloro analogue of the DBBA used by Cai to synthesize 7-armchair graphene nanoribbons (7-acGNR), as shown in Scheme 1.

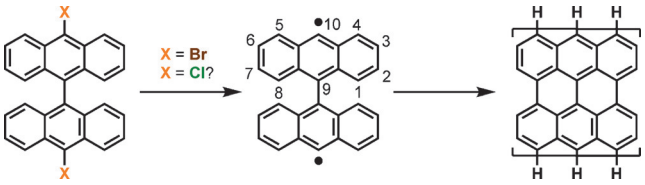

Scheme 1. Synthesis of 7-acGNR from bianthryl halides through subsequent Ullmann coupling and cyclodehydrogenation. Numbering is shown for a single anthryl unit.

We find that changing the halogen strongly impacts the course of the reaction: instead of the expected graphene nanoribbons, we observe the formation of fused oligo- and polybisanthenes (bisanthene being the cyclodehydrogenized form of bianthryl) with varying degrees of atomic order. This difference is proposed to stem from the stronger C–Cl bond allowing for cyclodehydrogenation prior to radical formation.

First, DCBA molecules were evaporated onto an Au(111) crystal held at room temperature. As is evident from the STM image shown in Figure 1a, a well-ordered self-assembled layer was observed. The apparent height (4.0 ± 0.5 Å) and

[*] P. H. Jacobse, Dr. I. Swart
Condensed Matter and Interfaces, Debye Institute for Nanomaterials Science, Utrecht University
PO Box 80000, 3508 TA Utrecht (The Netherlands)
E-mail: i.swart@uu.nl
P. H. Jacobse, A. van den Hoogenband, Dr. M.-E. Moret, Prof. R. J. M. Klein Gebbink
Organic Chemistry and Catalysis, Debye Institute for Nanomaterials Science, Utrecht University
Universiteitsweg 99, 3584 CG Utrecht (The Netherlands)
E-mail: m.moret@uu.nl

Supporting information for this article can be found under: http://dx.doi.org/10.1002/anie.201606440.

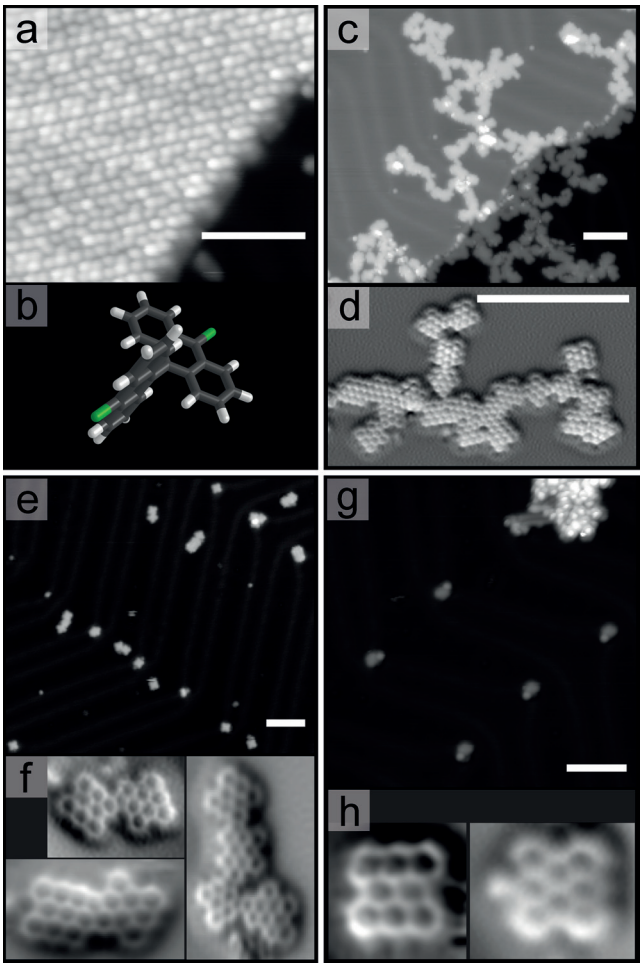

Figure 1. STM and AFM images of DCBA molecules on the Au(111) surface treated at different temperatures. a) Room temperature. b) Model of the DCBA. c) Heated to 360 °C. d) AFM of structures in (c). e) Heated to 200 °C. f) AFM on structures in e. g) Heated to 120 °C. h) AFM on structures in g. All scale bars are 5 nm.

periodicity (1.2 ± 0.2 nm) are consistent with a close packing of DCBA molecules. Interestingly, multiple crystal structures were identified within the monolayer, which we ascribe to variations in the three-dimensional orientation of DCBA molecules relative to each other. As shown in the Supporting Information, the structures could be interconverted by applying voltage pulses.

Subsequent slow heating of the sample from room temperature to 360 °C over the course of 1 h results in a large decrease of adsorbate concentration. The remaining molecules formed extensive disordered polymer-like chains, near the Au(111) step edges, as seen in Figure 1 c. These chains have a different conjugation than graphene nanoribbons.[11] The formation of disordered chains implies that the orientation and coupling of subsequent bisanthenes is random and that branching of the chains is prevalent. This is confirmed using sub-molecular resolution AFM images (Figure 1 d). This is in obvious contrast with the linear structures that result from radical–radical coupling of staggered bianthryl radical intermediates, as is the case for DBBA.

By having performed the assembly of DCBA in a slow-heating experiment, we rule out a possible temperature quenching effect: the hypothetical case that molecules are heated too quickly to a temperature at which they may undergo intramolecular reactions before having the chance to couple.[12] Hence, the rationale behind slow heating is that it maximizes the probability that all steps in the mechanism are traversed in the order of increasing activation energy while giving every single one of them enough time to occur before possibly being quenched by reactions that happen at higher temperature. Since both coupling and cyclodehydrogenation reactions must have occurred for the polybisanthene chains to form, it was decided to carry out the next experiments at lower temperatures, closer to the onset of various reactions.

When evaporating molecules onto Au(111) maintained at 200 °C, smaller, planar structures are observed. In AFM these were found to correspond to mostly monomers, dimers and oligomers of bisanthene (Figure 1 e). In the STM images, the vast majority of dimers appear as a structure where the two monomers are attached at a 34 ± 5 degree angle (based on 11 measurements). A few dimers feature a different angle and appear to be fused even more intricately. AFM (Figure 1 f) reveals both of these structures to be fused bisanthene dimers, both featuring the non-alternant fluoranthene-type motif, containing a single pentagon sandwiched between the two moieties. Similar attachments are seen in oligomers (Figure 1 d).

Evaporating molecules onto Au(111) heated to 120 °C results mostly in agglomerates of staggered molecules. In addition, some flat molecules were observed, particularly near the kink sites of the Au(111) herringbone reconstruction (Figure 1 g). Most of these flat species were identified as bisanthene, with a smaller fraction of monochlorobisanthene (Figure 1 h). At even lower temperatures, no flat molecules were observed, indicating that cyclodehydrogenation of bianthryl species does not take place.

The observation of monochlorobisanthene implies that the DBCA molecules first undergo cyclodehydrogenation and only then dehalogenation and polymerization. This order is reversed with respect to the order found for the bromo-analog (DBBA)[6,7a] (see Figure 2). This can be rationalized from the fact that the carbon–chlorine bond is stronger than the carbon–bromine bond.

When dehalogenation precedes cyclodehydrogenation, that is, the case of DBBA, bianthryl radicals are formed. The staggered geometry of bianthryl radicals is essential to alleviate the steric repulsion between the peri hydrogen atoms and allow for carbon–carbon coupling at the 10 and 10′ positions.[13] Only this coupling will result in well-defined graphene nanoribbons. When the order of the reaction is reversed, radical polymerization can only occur between planar species that are lying flat on the surface. Here the radical carbon atom is flanked by two peri-hydrogens, which pose a significant sterical difficulty for the radical to approach another molecule—particularly another radical. For the planar radical, the most accessible position is now the corner, as shown in Scheme 2. C–C bond formation at this position gives an intermediate bisanthenylbisanthene, which, when followed by cyclization, gives the dimeric structures that

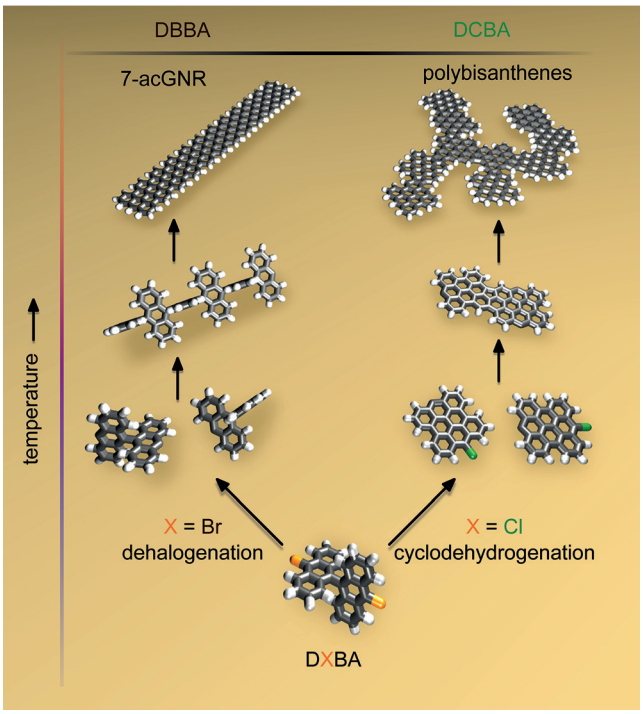

Figure 2. Mechanisms for the nanographene formation from dibromobianthryl (left) and dichlorobianthryl (right).

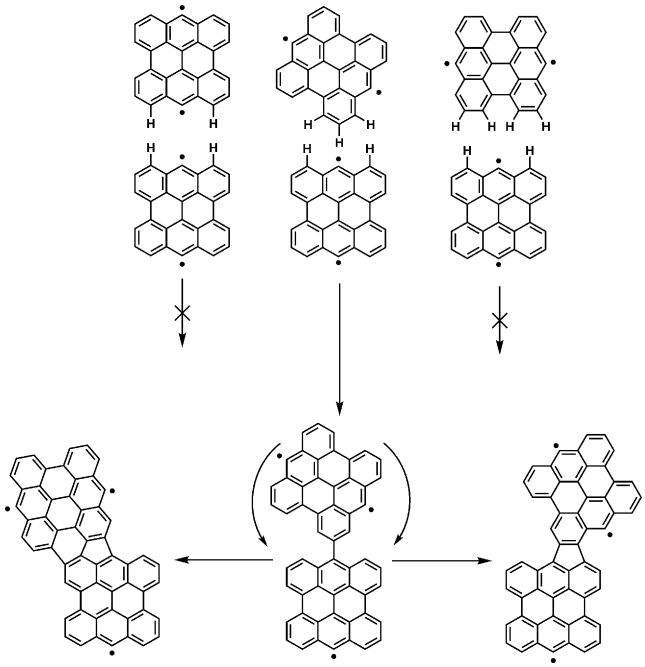

Scheme 2. Coupling mechanism for bisanthene radicals. Only hydrogens that play a role in the steric effect are shown explicitly. Radical-to-corner attack may create a bisanthenylbisanthene intermediate, which then cyclizes into either fused dimeric structure after pivoting to the left or to the right around this bond (as denoted by the curved arrows).

were resolved with AFM (Figure 1 f). The present data do not, however, allow us to resolve the exact mechanism of coupling. It may be that the hydrogen at the corner is lost during the bisanthenylbisanthene formation in a single step. Alternatively, the hydrogen may be removed from the corner by an initial abstraction through a first-generation radical, followed by radical–radical coupling to another bisanthene radical. Both hypothetical couplings will give rise to the same type of dimers. The dimer radicals may be passivated by H atoms or participate in further coupling steps to give oligo- and polybisanthenes. Since coupling can occur at every corner, ill-defined polybisanthene chains are formed. Upon increasing the temperature, also more indistinct radical coupling reactions can take place. Nevertheless, a significant amount of fluoranthene-type connections can be distinguished in the polybisanthenes. We conclude that the three-dimensional geometry of the intermediate radicals determines the regioselectivity in aryl–aryl bond formation.

Further evidence of the necessity of radical species in the coupling reactions was obtained from experiments with the non-halogenated 9,9′-bianthryl, as described in the Supporting Information (S1). Since this molecule cannot dehalogenate to form a radical, it is not expected to participate in coupling reactions. Indeed, no coupling products could be observed in experiments with bianthryl.

In summary, we investigated the Ullmann coupling of DCBA, an aryl chloride, on Au(111). In contrast to the coupling of the analogous bromide, highly branched structures were formed, which is due to an inversion of dehalogenation and cyclodehydrogenation steps. This changes the intermediate radicals from staggered bianthryl-type to planar bisanthene-type. Because of steric effects these undergo an alternative coupling reaction, giving rise predominantly to fluoranthene-type connections. We conclude that the geometry of the aryl radical, in combination with surface confinement determines the regioselectivity of C–C bond formation on surfaces. The notion that the reaction sequence in on-surface synthesis can be tuned by proper choice of halogen, combined with the importance of the geometry of reaction intermediates establishes new design criteria for the preparation of nanographenes and covalent organic frameworks. Specifically, the strong aryl chloride bond may be used to allow for intramolecular reactions before intermolecular couplings in cases where the analogous bromide gives the reverse order. Proper design of monomers may furthermore exploit the steric effects to generate the desired products in future syntheses.

Experimental Section

The compound 10,10′-dichloro-9,9′-bianthryl was synthesized via Suzuki coupling of 9-anthrylboronic acid[14] with 9-bromoanthracene, followed by chlorination of the intermediate 9,9′-bianthryl. See the Supporting Information for details.

The scanning probe experiments were carried out with a Scienta-Omicron LT STM/AFM with a commercially available qPlus sensor (quality factor of $Q \approx 30000$, a resonance frequency of $f_0 = 19500$ Hz and a peak-to-peak oscillation amplitude of approximately 2 Å), operating at 4.6 K. The molecules were thermally evaporated onto an Au(111) surface cleaned by several sputter and annealing cycles. All AFM images were acquired in constant height mode with CO terminated tips prepared using standard procedures.[15]

Acknowledgements

We gratefully acknowledge funding by a NWO Graduate Program and the Sector Plan Chemistry and Physics.

Keywords: atomic force microscopy · graphene nanoribbons · scanning tunnelling microscopy · surface synthesis · Ullmann coupling

How to cite: *Angew. Chem. Int. Ed.* **2016**, *55*, 13052 – 13055
Angew. Chem. **2016**, *128*, 13246 – 13249

[1] a) Q. Fan, J. M. Gottfried, J. Zhu, *Acc. Chem. Res.* **2015**, *48*, 2484 – 2494; b) M. El Garah, J. M. Macleod, F. Rosei, *Surf. Sci.* **2013**, *613*, 6 – 14; c) X. Zhang, Q. Zeng, C. Wang, *Nanoscale* **2013**, *5*, 8269 – 8287; d) L. Dong, P. N. Liu, N. Lin, *Acc. Chem. Res.* **2015**, *48*, 2765 – 2774; e) G. Franc, A. Gourdon, *Phys. Chem. Chem. Phys.* **2011**, *13*, 14283; f) J. Méndez, M. F. López, J. A. Martín-Gago, *Chem. Soc. Rev.* **2011**, *40*, 4578 – 4590; g) J. Björk, *J. Phys. Condens. Matter* **2016**, *28*, 083002; h) M. Lackinger, W. M. Heckl, *J. Phys. D* **2011**, *44*, 464011.

[2] a) K. J. Shi, D. W. Yuan, C. X. Wang, C. H. Shu, D. Y. Li, Z. L. Shi, X. Y. Wu, P. N. Liu, *Org. Lett.* **2016**, *18*, 1282 – 1285; b) M. Kittelmann, M. Nimmrich, R. Lindner, A. Gourdon, A. Kühnle, *ACS Nano* **2013**, *7*, 5614 – 5620; c) H. Zhang, J. H. Franke, D. Zhong, Y. Li, A. Timmer, O. D. Arado, H. Mönig, H. Wang, L. Chi, Z. Wang et al., *Small* **2014**, *10*, 1361 – 1368; d) M. Kittelmann, P. Rahe, M. Nimmrich, C. M. Hauke, A. Gourdon, A. Kühnle, *ACS Nano* **2011**, *5*, 8420 – 8425.

[3] a) C. Zhang, Q. Sun, H. Chen, Q. Tan, W. Xu, *Chem. Commun.* **2015**, *51*, 495 – 498; b) L. Grill, M. Dyer, L. Lafferentz, M. Persson, M. V. Peters, S. Hecht, *Nat. Nanotechnol.* **2007**, *2*, 687 – 691; c) Q. Fan, C. Wang, Y. Han, J. Zhu, J. Kuttner, G. Hilt, J. M. Gottfried, *ACS Nano* **2014**, *8*, 709 – 718; d) C. Sánchez-Sánchez, S. Brüller, H. Sachdev, K. Müllen, M. Krieg, H. F. Bettinger, A. Nicolaï, V. Meunier, L. Talirz, R. Fasel et al., *ACS Nano* **2015**, *9*, 9228 – 9235; e) L. Lafferentz, F. Ample, H. B. Yu, S. Hecht, C. Joachim, L. Grill, *Science* **2009**, *323*, 1193 – 1197; f) R. Gutzler, L. Cardenas, J. Lipton-Duffin, M. El Garah, L. E. Dinca, C. E. Szakacs, C. Fu, M. Gallagher, M. Vondráček, M. Rybachuk et al., *Nanoscale* **2014**, *6*, 2660 – 2668.

[4] a) J. A. Lipton-Duffin, O. Ivasenko, D. F. Perepichka, F. Rosei, *Small* **2009**, *5*, 592 – 597; b) M. Bieri, M.-T. Nguyen, O. Gröning, J. Cai, M. Treier, K. Aït-Mansour, P. Ruffieux, C. A. Pignedoli, D. Passerone, M. Kastler et al., *J. Am. Chem. Soc.* **2010**, *132*, 16669 – 16676; c) G. Eder, E. F. Smith, I. Cebula, W. M. Heckl, P. H. Beton, M. Lackinger, *ACS Nano* **2013**, *7*, 3014 – 3021; d) S. Schlögl, W. M. Heckl, M. Lackinger, *Surf. Sci.* **2012**, *606*, 999 – 1004.

[5] a) L. Lafferentz, V. Eberhardt, C. Dri, C. Africh, G. Comelli, F. Esch, S. Hecht, L. Grill, *Nat. Chem.* **2012**, *4*, 215 – 220; b) J. Eichhorn, D. Nieckarz, O. Ochs, D. Samanta, M. Schmittel, P. J. Szabelski, M. Lackinger, *ACS Nano* **2014**, *8*, 7880 – 7889; c) J. Eichhorn, T. Strunskus, A. Rastgoo-Lahrood, D. Samanta, M. Schmittel, M. Lackinger, *Chem. Commun.* **2014**, *50*, 7680 – 7682; d) J. Björk, F. Hanke, S. Stafstrom, *J. Am. Chem. Soc.* **2013**, *135*, 5768 – 5775; e) K. J. Shi, X. Zhang, C. H. Shu, D. Y. Li, X.-Y. Wu, P. N. Liu, *Chem. Commun.* **2016**, *52*, 8726 – 8729.

[6] J. Cai, P. Ruffieux, R. Jaafar, M. Bieri, T. Braun, S. Blankenburg, M. Muoth, A. P. Seitsonen, M. Saleh, X. Feng et al., *Nature* **2010**, *466*, 470 – 473.

[7] a) A. Batra, D. Cvetko, G. Kladnik, O. Adak, C. Cardoso, A. Ferretti, D. Prezzi, E. Molinari, A. Morgante, L. Venkataraman, *Chem. Sci.* **2014**, *5*, 4419 – 4423; b) L. Massimi, O. Ourdjini, L. Lafferentz, M. Koch, L. Grill, E. Cavaliere, L. Gavioli, C. Cardoso, D. Prezzi, E. Molinari et al., *J. Phys. Chem. C* **2015**, *119*, 2427 – 2437.

[8] a) C. Bronner, J. Björk, P. Tegeder, *J. Phys. Chem. C* **2015**, *119*, 486 – 493; b) S. Blankenburg, J. Cai, P. Ruffieux, R. Jaafar, D. Passerone, X. Feng, K. Müllen, R. Fasel, C. A. Pignedoli, *ACS Nano* **2012**, *6*, 2020 – 2025; c) J. Björk, S. Stafström, F. Hanke, *J. Am. Chem. Soc.* **2011**, *133*, 14884.

[9] L. Talirz, H. Söde, J. Cai, P. Ruffieux, S. Blankenburg, R. Jafaar, R. Berger, X. Feng, K. Müllen, D. Passerone et al., *J. Am. Chem. Soc.* **2013**, *135*, 2060 – 2063.

[10] a) Y.-C. C. Chen, D. G. de Oteyza, Z. Pedramrazi, C. Chen, F. R. Fischer, M. F. Crommie, *ACS Nano* **2013**, *7*, 6123 – 6128; b) R. R. Cloke, T. Marangoni, G. D. Nguyen, T. Joshi, D. J. Rizzo, C. Bronner, T. Cao, S. G. Louie, M. F. Crommie, F. R. Fischer, *J. Am. Chem. Soc.* **2015**, *137*, 8 – 11; c) S. Kawai, S. Saito, S. Osumi, S. Yamaguchi, A. S. Foster, P. Spijker, E. Meyer, *Nat. Commun.* **2015**, *6*, 8098; d) A. Kimouche, M. M. Ervasti, R. Drost, S. Halonen, A. Harju, P. M. Joensuu, J. Sainio, P. Liljeroth, *Nat. Commun.* **2015**, *6*, 10177; e) P. Ruffieux, S. Wang, B. Yang, C. Sanchez, J. Liu, T. Dienel, L. Talirz, P. Shinde, C. A. Pignedoli, D. Passerone et al., *Nature* **2015**, *531*, 15.

[11] M. Koch, F. Ample, C. Joachim, L. Grill, *Nat. Nanotechnol.* **2012**, *7*, 713.

[12] B. Cirera, N. Gimenez-Agullo, J. Bjork, F. Martinez-Pena, A. Martin-Jimenez, J. Rodriguez-Fernandez, A. M. Pizarro, R. Otero, J. M. Gallego, P. Ballester et al., *Nat. Commun.* **2016**, *7*, 11002.

[13] T. Kaneko, N. Tajima, T. Ohno, *Jpn. J. Appl. Phys.* **2016**, *55*, 06GF05.

[14] a) E. Clar, *Ber. Dtsch. Chem. Ges.* **1939**, *72*, 1645 – 1649; b) S. K. Talapatra, S. Chakrabarti, A. K. Mallik, B. Talapatra, *Tetrahedron* **1990**, *46*, 6047 – 6052.

[15] L. Gross, F. Mohn, N. Moll, P. Liljeroth, G. Meyer, *Science* **2009**, *325*, 1110 – 1114.

Received: July 3, 2016
Published online: September 16, 2016

